Available online at www.sciencedirect.com
ScienceDirect
Biomaterials 28 (2007) 4608–4618
Biomaterials
www.elsevier.com/locate/biomaterials

Supramolecular crafting of cell adhesion

Hannah Storrie[a], Mustafa O. Guler[a], Suha N. Abu-Amara[b], Tova Volberg[b], Mukti Rao[a], Benjamin Geiger[b], Samuel I. Stupp[a,c,d,*]

[a]Department of Chemistry, Northwestern University, Evanston, IL 60208, USA
[b]Department of Molecular Cell Biology, Weizmann Institute of Science, Rehovot 76100, Israel
[c]Department of Materials Science and Engineering, Northwestern University, Evanston, IL 60208, USA
[d]Feinberg School of Medicine, Northwestern University, Evanston, IL 60208, USA

Received 12 June 2007; accepted 13 June 2007
Available online 27 July 2007

Abstract

The supramolecular design of bioactive artificial extracellular matrices to control cell behavior is of critical importance in cell therapies and cell assays. Most previous work in this area has focused on polymers or monolayers which preclude control of signal density and accessibility in the nanoscale filamentous environment of natural matrices. We have used here self-assembling supramolecular nanofibers that display the cell adhesion ligand RGDS at van der Waals density to cells. Signal accessibility at this very high density has been varied by changes in molecular architecture and therefore through the supramolecular packing of monomers that form the fibers. We found that branched architectures of the monomers and the consequent lower packing efficiency and additional space for epitope motion improves signaling for cell adhesion, spreading, and migration. The use of artificial matrices with nanoscale objects with extremely high epitope densities could facilitate receptor clustering for signaling and also maximize successful binding between ligands and receptors at mobile three-dimensional interfaces between matrices and cells. Supramolecular design of artificial bioactive extracellular matrices to tune cell response may prove to be a powerful strategy in regenerative medicine and to study biological processes.

Keywords: Cell adhesion; Cell signaling; Hydrogel; Self-assembly

1. Introduction

The supramolecular design of artificial extracellular matrices is key to our understanding of cell–matrix interactions, and of great importance for the future of regenerative medicine. The most common target has been the use of a matrix to activate receptor-mediated biological adhesion mechanisms since they are critical to cell survival and function. Biological cell adhesion to the extracellular matrix (ECM) commonly occurs via binding of integrin receptors to specific epitopes present on the surface of ECM proteins such as fibronectin, leading to the formation of focal adhesions (FAs) and related contacts [1,2]. These adhesions consist of protein assemblies that serve to connect the cell interior to the external environment [3–11]. Upon binding of an integrin to its ligand, additional integrins, adapter proteins and cytoskeletal components are recruited to the nascent adhesion, forming a structurally defined FA. The cytoplasmic proteins that are recruited are of two major types, namely scaffolding proteins, which provide the mechanical link between integrins and the actin cytoskeleton, and signaling molecules that trigger and transduce adhesion-dependent cues [3,4,6–14]. A common ligand present on several ECM proteins is the peptide sequence arginine-glycine-aspartic acid (RGD) [15,16], which is sufficient for triggering cell adhesion.

Most previous work on artificial ECMs has focused on the design of polymeric matrices with attributes such as biodegradable backbones [17,18], ability to form

*Corresponding author. Department of Materials Science and Engineering, Northwestern University, Cook Hall, Room 1127, 2220 Campus Drive, Evanston, IL 60208, USA. Tel.: +1 847 491 3002; fax: +1 847 491 3010.
E-mail address: s-stupp@northwestern.edu (S.I. Stupp).

0142-9612/$ - see front matter © 2007 Elsevier Ltd. All rights reserved.
doi:10.1016/j.biomaterials.2007.06.026

gels [19–22], or functionalization with bioactive peptides [23,24] most notably RGD [25,26]. Massia and Hubbell first showed that RGD ligand density can affect cell adhesion using peptide coated glass surfaces, reporting complete fibroblast spreading on RGD-grafted glass surfaces at a ligand density of 10 fmol/cm^2 (440 nm ligand spacing) and FA formation occurring at an average ligand density of 1 fmol/cm^2 (140 nm ligand spacing) [27–29]. In other work, a lateral spacing between epitopes of 50–70 nm has also been shown to be critical for FA formation [30]. Subsequent studies in different cell types have shown that while there is a maximum density above which further enhancement of cell spreading is no longer observed, it is often higher than that observed by Massia and Hubbell (30 fmol/cm^2 for myoblasts [31]) [32–34]. Studies by Griffith et al. and Mooney et al. using polymers grafted with cell adhesion epitopes have shown that at a given ligand density, cell adhesion can be modulated by the spatial arrangement of the ligands [35,36]. For example, forming arrays of clustered RGD ligands by coupling multiple epitopes to a single polymer chain enhances cell attachment as compared to distributing the same number of RGD ligands by coupling one epitope per polymer chain [35]. These studies indicate that while a sufficient number of adhesion epitopes are required to sustain cell attachment, the nanoscale presentation of those ligands is also important in regulating the attachment of cells to artificial matrices.

The supramolecular details of biological signal display for optimal cell–matrix interactions in vitro and in vivo remain largely unclear. Supramolecular structure in the ECM is directly linked to epitope density and dynamics, and it is relevant in cell–matrix interactions given the importance of receptor clustering in signaling and the mechanical softness of the interface where cells meet their matrix. Previously studied polymeric systems are inherently disordered, which precludes control of parameters such as the local supramolecular structure or the density and spatial orientation of bioactive signals. Self-assembling monolayers, which can present highly ordered ligand arrays, have been studied, [37,38] but these systems do not mimic the three-dimensional (3D) filamentous environment of extracellular matrices. In ordered monolayers it is also difficult to change signal accessibility without diluting the signal with mixtures of short and long molecules.

In this work we probe the interactions of cells with supramolecular peptide amphiphile (PA) nanofibers in which the display of RGD epitopes can be altered at extremely high ligand density by changing their local dynamics either through the architecture of molecules or dilution of the epitopes. The nanofibers are cylindrical in shape and have a very high aspect ratio and therefore are able to mimic the soft fibrous environment that naturally surround cells (diameters on the order of 6–8 nm and lengths easily approaching microns) [39–43]. The fibers, as opposed to monolayers, are able to maintain essentially constant epitope densities with different degrees of epitope packing as a result of sterics and therefore, signal accessibility can be examined in three dimensions. This versatility as one varies the sterics of molecular architecture of monomers is a virtue of structures with curvature that are not pinned on a lattice. These nanostructures are formed from molecules containing an aliphatic tail covalently linked to a peptide segment terminated with the bioactive RGD sequence. Therefore every single molecule in the supramolecular assembly displays an epitope, and cells can explore an environment with essentially van der Waals densities of bioactive signals. This approach also presents to cells a well-defined density of epitopes which is difficult to achieve when grafting epitopes to surfaces or substituting polymers. Upon self-assembly from aqueous solution, the cylindrical nanofibers display their bioactive sequences perpendicular to the long axis of the nanostructure, and inter-fiber contacts create a network that functions as an artificial ECM for cells. In the current study, we have utilized PAs with different covalent architectures in the segment that presents the bioactive epitope, allowing us to explore the effects of epitope dynamics through variations in supramolecular packing of PA molecules, while maintaining high epitope density. Dense tight packing of epitopes with little mobility is achieved with PA molecules with linear architecture, and less efficient packing resulting in more mobile epitopes with branched or cyclic architectures (see Fig. 1) [44]. We examine here the behavior of cells on PA nanofibers to determine if cells can sense and respond to differences in epitope dynamics as supramolecular packing is modified.

2. Materials and methods

2.1. Preparation of peptide amphiphiles

Details of linear and branched PA synthesis have been reported elsewhere [44,45].

2.2. Cell culture

3T3 fibroblasts were maintained in phenol red-free Dulbecco's modified eagle medium (DMEM) supplemented with 10% fetal bovine serum (FBS) and penicillin/streptomyocin. REF52, B16, and MDA 231 cells were maintained in DMEM media containing phenol red supplemented as for 3T3 fibroblasts.

2.3. Cover slip preparation

Ethanol sterilized number 1 glass cover slips were drop cast with 0.01 wt% solutions of PAs, fibronectin, and poly-D-lysine (PDL) for 3 h, placed in a sterile 24 well culture dish, and then rinsed with phosphate buffered saline (PBS) and allowed to dry overnight before use. For experiments with REF 52 and B16 cells, glass bottom 13 mm culture dishes coated in the same manner as glass cover slips were used.

2.4. Two-dimensional (2D) cell adhesion assays

3T3 fibroblasts were incubated in FBS-free DMEM media supplemented with 4 mg/mL bovine serum albumin, and 50 mg/mL cyclohexamide for 1 h prior to use. Cells were removed from culture flasks with

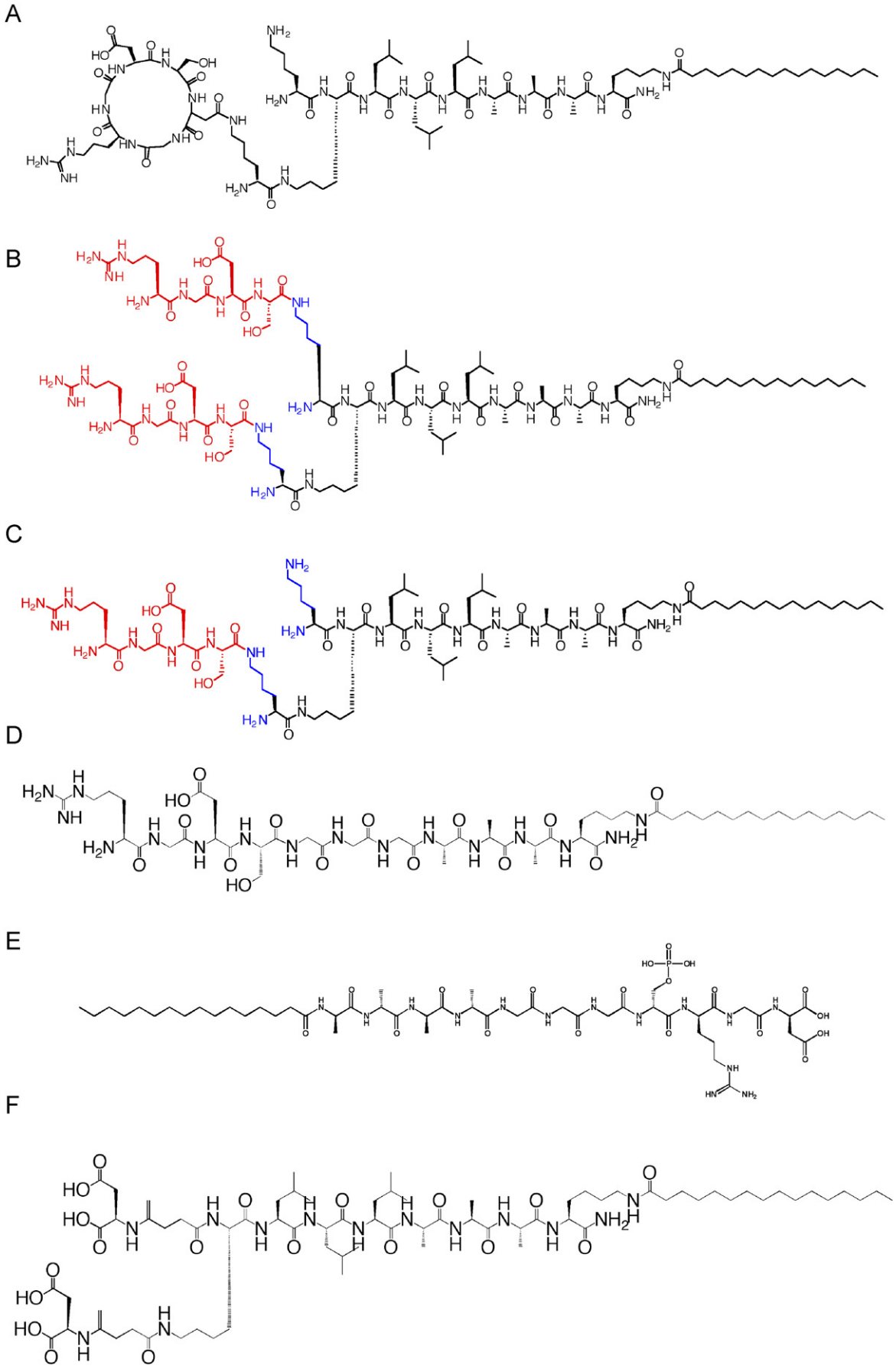
A
B
C
D
E
F

trypsin/EDTA and resuspended in FBS-free DMEM at a concentration of 1.0×10^4 cells/mL; 1 mL of the cell suspension was added to each well of a 24 well culture plate containing a coated cover slip. Cells were cultured for 4–6 h at 37 °C. Cell adhesion was assayed quantitatively with CyQuant (Molecular Probes) using fluorescence detection in white walled, clear bottom, 96 well plate on a Molecular Devices Gemini EM model fluorescence plate reader with excitation at 480 nm and emission monitored at 520 nm. Phase contrast images of cells cultured in the adhesion experiments were collected at 200× using a Nikon TE200 inverted microscope with a SPOT RT CCD camera controlled by Metamorph 1.0 software package. For cell spreading experiments, at least 50 cells on each PA were counted from four different samples and the percent of spread cells was recorded.

2.5. Soluble GRGDS competition assay

3T3 fibroblasts were incubated for 1 h in FBS-free DMEM containing 0.1 mg/mL GRGDS peptide prior to use; 1.0×10^4 cells were added to each well of a 24 well culture plate containing a coated cover slip. Cells were maintained in FBS-free DMEM with soluble GRGDS for 4–6 h. Coverslips were processed as for adhesion experiments and assayed with CyQuant.

2.6. Imaging of FA formation

REF 52 cells expressing YFP-paxillin and B16 cells expressing GFP-β_3 integrin were cultured in phenol red- and riboflavin-free DMEM media and plated at densities between 1×10^4 and 1×10^6 cells/mL on PA coated glass coverslips embedded in 13 mm culture dishes. Cells were cultured for 4 h and then either imaged live or fixed with 3% paraformaldehyde. Images were taken with the DeltaVision system on an Olympus IX70 inverted microscope. Image acquisition and processing were controlled by a Silicon Graphics workstation model O2 using the Resolve3D and Priism software packages.

2.7. RGD dilution assays

RGD-containing PAs were diluted in solution with a diluent PA containing a branched headgroup with only two aspartic acid groups. Solutions containing 100%, 90%, 70%, 50%, 30%, 10%, 5%, 2.5% and 0% RGD-containing PA by volume were drop cast onto cover slips in the same manner as for the adhesion experiments. Cells were cultured under the same conditions as for the previous adhesion studies and amount of cell adhesion was assayed using CyQuant.

2.8. 3D cell migration assays

MDA 231 cells were maintained in DMEM media supplemented with 10% FBS and penicillin/streptomycin. Prior to plating on gels, resuspended in phenol red and riboflavin free DMEM supplemented with l-glutamine, penicillin/streptomycin, and HEPES buffer. Gels were formed in glass bottomed 96 well plates and cured for at least 1 h before use. Cells were plated at a concentration of 1000 cells/mL and maintained in a temperature-regulated chamber for live-cell imaging over time. Time lapse images were collected on an Olympus IX70 inverted microscope with a Proscan automated stage control, Quantix CCD camera controlled by Resolve 6D software running on a Zeon PC computer. A 10 mW HeNe laser was used for autofocus control.

3. Results and discussion

3.1. 2D cell adhesion and spreading

2D cell adhesion and spreading experiments were carried out using as the substrate supramolecular nanofibers formed by the molecules shown in Fig. 1 cast on glass cover slips. These self-assembling molecules form nanofibers by self-assembly from aqueous solutions. We investigated two types of molecules, linear and branched PAs, with branched ones presenting either one or two RGDS epitopes in linear or cyclic form (See Fig. 2). Cells examined for cell attachment, spreading, and FA formation were maintained in serum-depleted medium, supplemented with protein synthesis inhibitor, to block secretion of adhesion proteins. Fibroblast attachment and spreading was found to be dependent on the type of PA molecule used for to form the supramolecular nanofibers (Figs. 3(A) and (B)). Enhanced cell attachment and spreading was observed on nanofibers formed by branched PAs compared to linear ones, and, as one might expect, branched PA nanofibers presenting a single RGDS epitope with D configuration exhibit less cell attachment than the corresponding nanofibers with L configuration [46]. Interestingly, in spite of the similar concentration of epitopes presented by the various supramolecular nanofibers (effectively van der Waals packing of epitopes), we observed significant differences in the number of adherent and spread cells. Nanofibers formed from branched PA molecules led to enhanced cell attachment and spreading as compared to linear PA nanofibers, and supramolecular fibers formed by the PA monomer containing a cyclic RGD peptide in branched architecture showed significantly higher cell spreading than a fibronectin control. All PAs showed enhanced cell adhesion compared to a PDL negative control. Among nanofibers formed from branched PAs, cell adhesion was dependent both on ligand density and ligand affinity. Varying the number of linear RGDS epitopes per molecule from one to two resulted in greater cell adhesion to the substrate, however, a branched PA containing a single high-affinity cyclic RGDS epitope led to to enhanced cell adhesion relative to the branched PA containing two linear epitopes.

The specificity of enhanced cell attachment was assayed by adding a soluble GRGDS peptide to the cell culture media to compete for integrin receptor adhesion with the supramolecular nanofibers. Cell attachment was decreased on nanofibers formed by branched PA molecules, while no decrease was observed for molecules bearing the epitope in linear architecture or in molecules containing the D-enantiomer of the epitope. These data strongly suggested that attachment and spreading of cells in the branched systems containing RGDS was mediated

Fig. 1. Chemical structure of branched and linear PAs. (A)–(C) Branched PAs with one cyclic RGDS epitope (A), two RGDS epitope (B), or one RGDS epitope (C). (D) Positively charged linear PA with one RGDS epitope. (E) Negatively charged linear PA with one RGD epitope, and (F) diluent branched PA containing two aspartic acid residues.

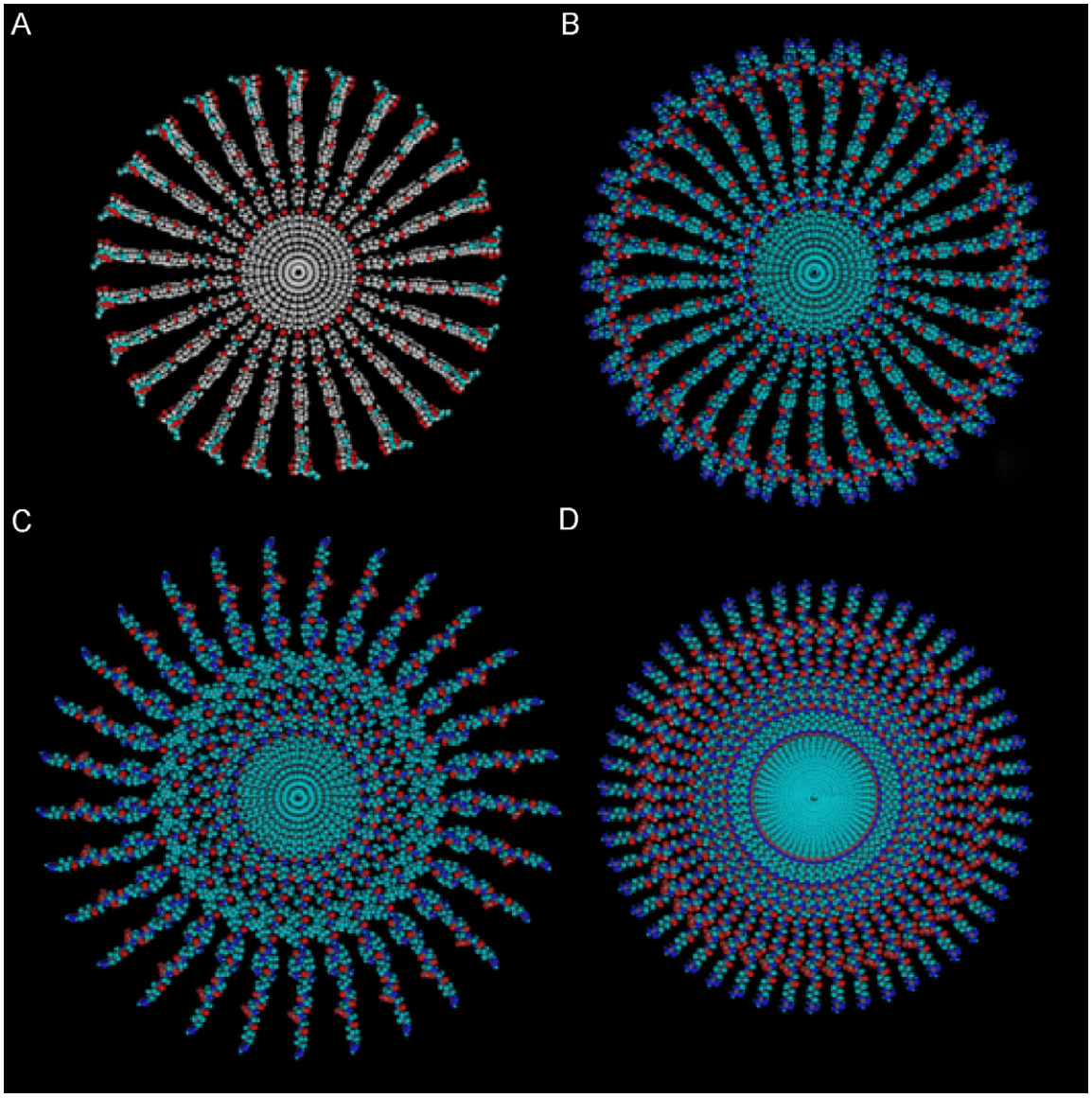

Fig. 2. Cross-sections of PA nanofibers formed from branched and linear PA molecules. (A) Branched PA with one cyclic RGDS epitope, (B) branched PA with two RGDS epitopes, (C) branched PA with one RGDS epitope, and (D) linear PA with one RGD epitope.

by the molecular epitope presented by the nanofibers, and was not the result of nonspecific forces of electrostatic or other origins. We have previously demonstrated the specific binding of avidin to a biotin-presenting branched PA, and that streptavidin–biotin binding is enhanced in branched PA nanofibers as compared to linear PA nanofibers [44]. While cell–nanofiber interactions are more complex than biotin–avidin binding, these systems provide physical and independent evidence of greater accessibility of the epitope for protein binding in branched PA systems. The data obtained here indicates that greater epitope accessibility is linked to supramolecular packing in the nanostructures, which leads to enhanced cell attachment and spreading.

The effects of PA architecture on FA formation were observed to confirm the link between cell binding and presentation of RGDS ligands by the nanofibers. The formation of FAs was observed directly in cells stably transfected with fluorescent cell adhesion fusion proteins, namely YFP-paxillin and GFP-β_3 integrin. B16 human melanoma cells expressing GFP-β_3 integrin and rat embryonic fibroblasts (REF 52) expressing YFP-paxillin were cultured in complete media on branched PA nanofibers. The expected distinct fluorescent patterns indicative of FA formation were observed in both cell types. B16 cells expressing GFP-β_3 integrin reveal small, bright spots of fluorescence on the leading edge of the cells as a result of β_3 integrin clustering (Figs. 4(A)–(F)) [3,47,48]. These spots were observed on cells cultured on all supramolecular fibers formed by branched PAs, and not on those composed of linear monomers or the similar PA molecules with D-isomers of the epitope. Also in branched PAs REF 52 cells show an organization of paxillin inside the cell that extends beyond integrins clustered at the cell edge (Figs. 4(G)–(L)) [49]. On linear nanofibers, punctuate

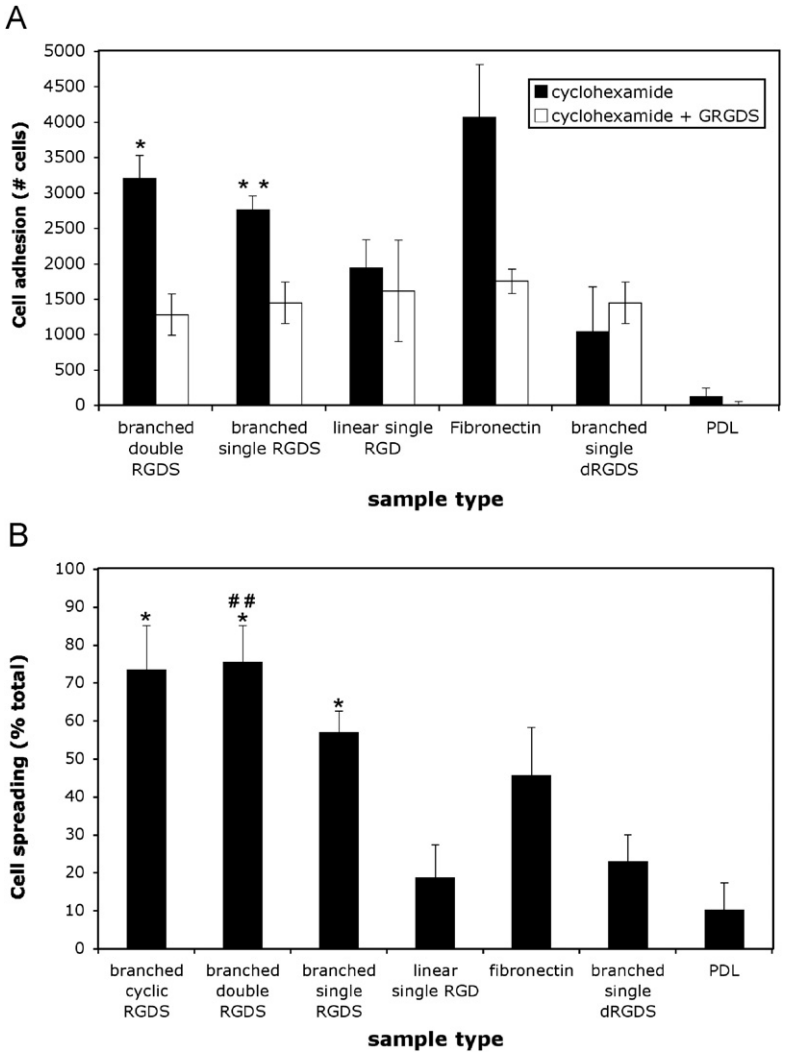

Fig. 3. Differential adhesion and spreading of 3T3 fibroblasts on branched and linear PAs. (A) Cell attachment in presence of cyclohexamide or cyclohexamide and soluble GRGDS. *By ANOVA analysis, branched PA containing two RGDS epitopes promotes significantly greater cell attachment as compared to branched PA with either one RGDS epitope, or one D-RGDS, and a linear PA ($p<0.05$) and **branched PA containing one RGDS epitope promotes greater cell attachement than either a branched PA containing one D-RGDS epitope or a linear PA ($p<0.01$). (B) Degree of cell spreading in presence of cyclohexamide. *By ANOVA analysis all branched PAs lead to significantly more cell spreading than linear PA or PA containing D-isomer ($p<0.05$) and $^{\#\#}$branched PA containing two RGDS epitopes promotes significantly more cell spreading than branched PA containing one RGDS epitope ($p<0.05$).

fluorescence is observed in both cell types, however, this fluorescence lacks the high definition of fully formed FAs as observed in branched systems. This may be the result of adhesions mediated by fibronectin present in the media and not by the supramolecular nanofibers. The effect is particularly pronounced in REF 52 cells expressing YFP-paxillin. The observation of well-defined FAs on substrates containing supramolecular nanofibers formed by branched molecules is consistent with the cell attachment and cell spreading data discussed previously.

The assays for cell adhesion demonstrate that cell adhesion to nanofibers displaying RGDS is integrin-mediated and can be modulated at high ligand density by controlling the ligand architecture. We calculated the average density of RGDS per unit area in branched and linear PA nanofibers using a previously reported method (Table 1) [43], and all densities are orders of magnitude greater than the maximum density of 10 fmol/cm^2 determined by Massia and Hubbell [28], yet we still observe differential cell adhesion and spreading among different PA nanostructures. In addition to the greater epitope mobility and accessibility in cyclic RGDS nanofibers due to less efficient supramolecular packing, the observed enhancement on these substrates may be due to the increased affinity of cells for the cyclic ligand which mimics the RGDS loop in fibronectin [50]. It is not clear why there is an increased adhesion observed in branched PAs containing two as opposed to one RGDS epitope since both are expected to exhibit similar dynamics and therefore accessibility to cells based on supramolecular packing. It is possible that charge repulsion between the two epitopes in the same molecule increases ligand accessibility at

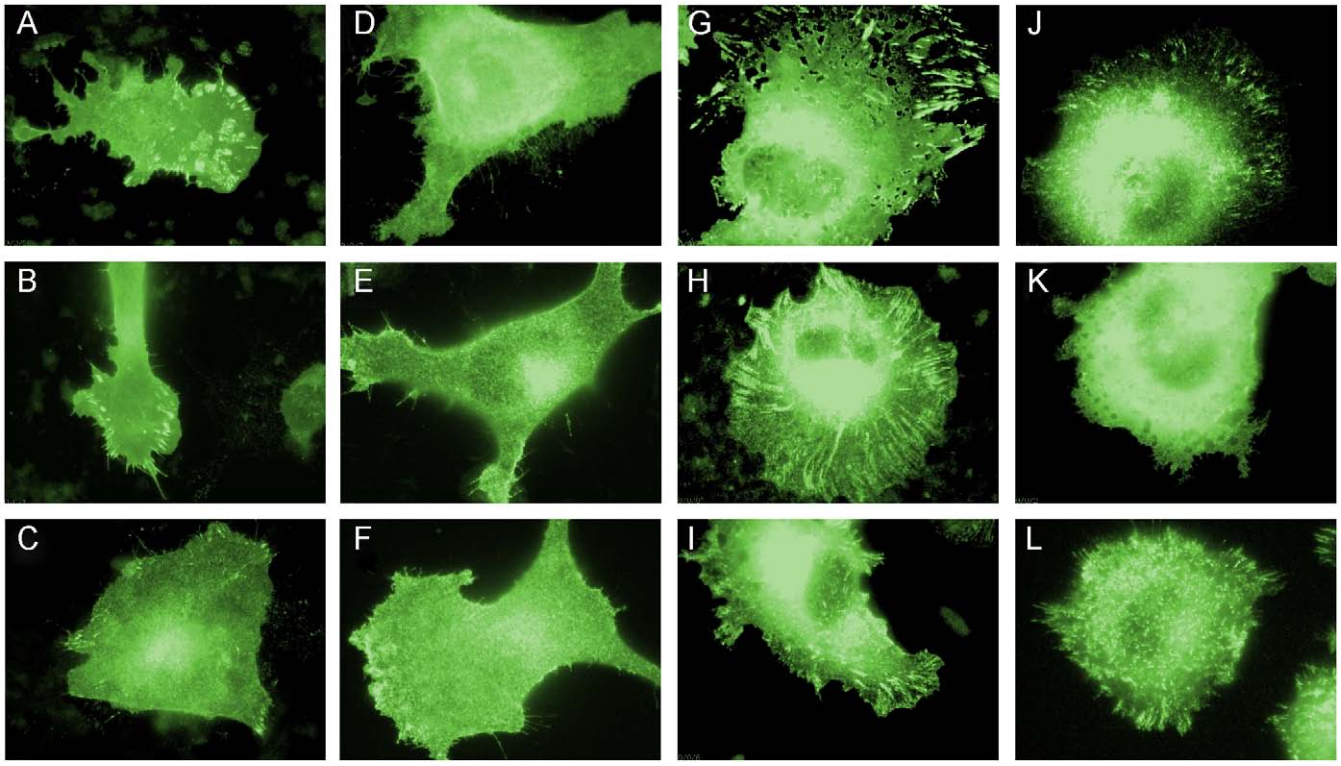

Fig. 4. Observation of focal adhesion formation. (A)–(F) B16 cells expressing GFP-β_3 integrin cultured on coverslips coated with (A) branched PA with one cyclic RGDS, (B) branched PA with two RGDS, (C) branched PA with one RGDS, (D) branched PA with one D-RGDS, (E) linear PA with one RGDS, and (F) linear PA with one RGD showing punctate fluorescene (arrowheads) indicative of FA formation. (G)–(L) REF52 cells expressing YFP-paxillin cultured on coverslips coated with (G) branched PA with one cyclic RGDS, (H) branched PA with two RGDS, (I) branched PA with one RGDS, (J) branched PA with one D-RGDS, (K) linear PA with one RGDS, and (L) linear PA with one RGD showing paxillin fluorescence (arrows) in FA assemblies.

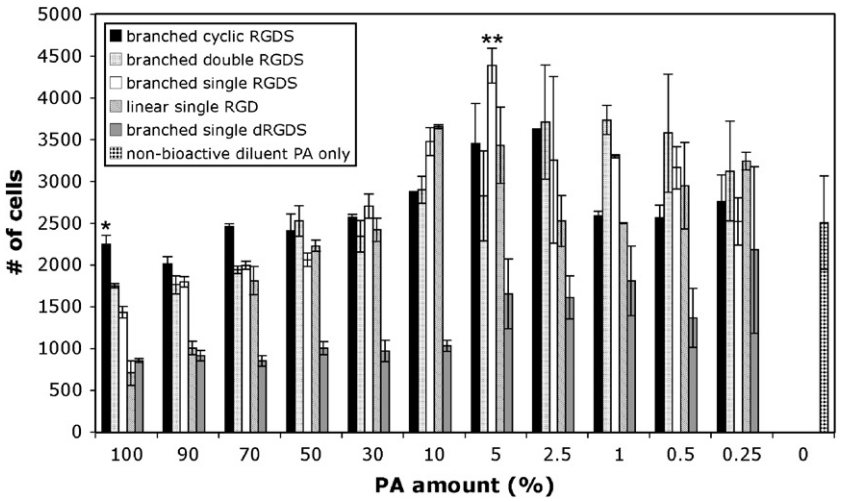

Fig. 5. Effect of RGDS dilution with diluent PA on adhesion of 3T3 fibroblasts cultured on coverslips coated with branched PAs containing either one cyclic RGDS, two RGDS, one RGDS, or one D-RGDS and a linear PA containing one RGD. *By ANOVA analysis branched PA containing cyclic RGDS promotes more cell attachment than all other PAs ($p<0.01$) and **maximum cell attachment is achieved with 5% branched single RGDS PA ($p<0.05$).

high density. Overall our results in this work are consistent with our previously reported observation of increased bioactivity of nanofibers formed by nanofibers of branched PA molecules in an in vitro assay for bladder tissue regeneration [51].

To further investigate the effect of molecular architecture on RGDS ligand accessibility and affinity, a series of epitope dilution experiments were performed (Fig. 5). Branched PAs were mixed with a diluent PA (Fig. 1), a branched aspartic acid PA (D-PA) that does not contain

Table 1
Density of RGDS in branched PA nanofibers

PA	# Molecules radially	Fiber diameter (nm)	Density (pmol/cm^2)
Branched cyclic RGDS	25	9	129
Branched double RGDS[a]	28	9	325
Branched single RGDS	28	9	162
Linear single RGD/S[b]	50	9	1178

[a]Two RGDS epitopes per molecule.
[b]Assumed to be the same for linear single RGDS and linear single RGD.

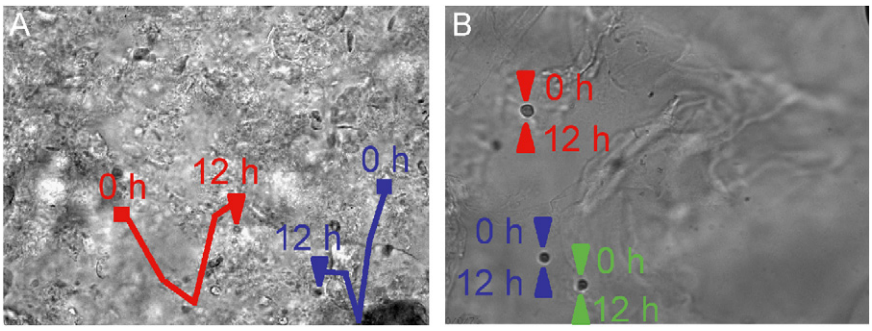

Fig. 6. Migration of MDA 231 cells through PA gels. (A) Migration paths of two individual cells (red and blue) through a gel formed from a branched PA with one RGDS epitope. (B) Migration paths of three individual cells (red, blue, and green) through a gel formed from a linear PA with one RGD epitope.

any cell-binding epitopes, but contains aspartic acid residues to promote electrostatic mixing of these negatively charged amino acids with the positively charged branched PAs. This approach to mix PA molecules in nanofibers was previously proposed by our laboratory [52] and circular dichroism spectra indicate co-assembly given the unique secondary structure in these nanofibers (data not shown). The diameter of the nanofiber decreases as the ratio of diluent PA to epitope-bearing PA increases, which allows the epitope to extend beyond the surface of the fiber. Previous work on monolayers has shown that extension of the epitope beyond the surface is effective to increase integrin-mediated cell attachment [53,54]. Therefore, it is not expected that the electrostatic influence of the diluent PA would play a significant role on cell attachment until the concentration of epitope-bearing PA molecules is too low to support integrin-mediated adhesion. Dilution led to an increase in cell attachment in all PAs (with the exception of the branched PA containing the D-isomer of the epitope) that was dependent on the architecture of the PA molecule. All branched PAs displayed a maximum adhesion at similar RGDS concentrations (8.1 pmol/cm^2 for a single RGDS epitope, 3.25 pmol/cm^2 for two RGDS epitopes and 3.22 pmol/cm^2 for cyclic RGDS), while maximum adhesion was observed for the linear PA at 120 pmol/cm^2. In all cases, the maximum adhesion was still observed at an RGDS concentration much higher than the previously reported ligand concentration required for cell attachment [28]. This confirms that cell attachment at low RGDS concentrations was integrin-mediated (not dependent on electrostatics) and further indicates the importance of epitope dynamics and accessibility to cell signaling. In linear PA nanofibers, one expects more interactions through hydrogen bonding among epitopes relative to branched systems, therefore, maximum adhesion in the mixed linear systems would require a higher RGDS concentration than in branched systems. Additionally, cell adhesion showed a greater enhancement with dilution on PA nanofibers with little ligand accessibility in the absence of dilution. Linear PA molecules showed a five-fold increase in the amount of cell adhesion with dilution, while the branched PA containing a cyclic RGDS epitope showed only a modest increase (a factor of 1.6). In branched nanofibers, the nature of supramolecular packing and consequent dynamics enables ligand accessibility to cells in spite of the high concentrations, while tighter packing in the linear PA molecules limits ligand accessibility at high concentrations.

3.2. 3D cell adhesion and migration

Time lapse imaging of cell migration in 3D PA gels was studied using highly migratory MDA231 human mammary carcinoma cells. Cells were encapsulated in either branched or linear PA gels, and migration was only observed in gels formed by branched PA molecules. Fig. 6(A) shows the migration paths of MDA231 cells inside a gel formed from a branched PA containing a single RGDS epitope. Over 12 h, multiple cells were observed in the field of view, and cells migration occurs in the x, y, and z directions. Cell migration is characterized by attachment of one edge of a rounded cell to the gel by the extension of cellular

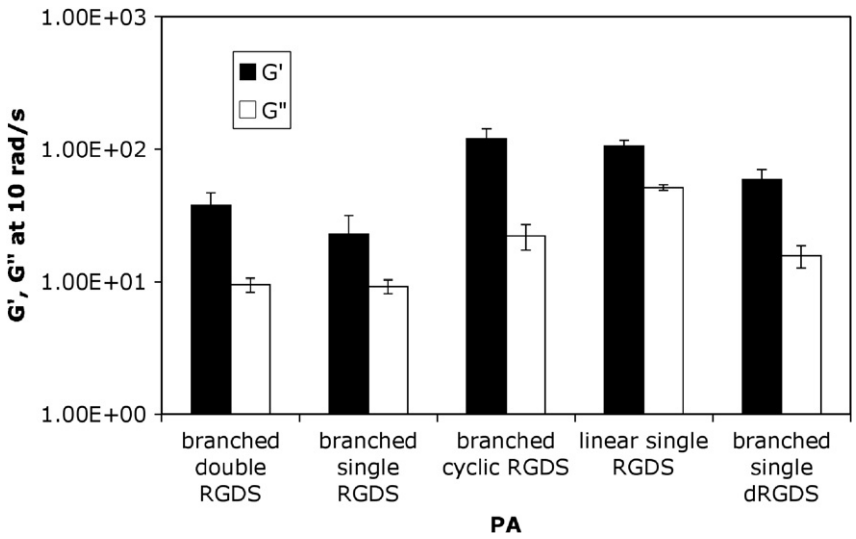

Fig. 7. Gel stiffness of PAs determined by oscillating rheometry.

processes, followed by the stretching and flattening of the cell body. The cell returns to a rounded state by pulling the trailing edge of the cell towards the leading edge, leading to movement within the gel. The cell repeats this cycle of extension and rounding to move through the gel in a manner largely similar to migration patterns observed in 2D culture. As cells migrate through the gel they appear to pull on it, causing movement of entire sections of the gel carried by the cell as they move. This pattern of migration, which has previously been observed for MDA 231 cells encapsulated in collagen gels, is indicative of integrin-mediated cell migration [55]. Cells can also be observed interacting with contours of the gel, and migrating along edges present in the gel. Some cells do fail to migrate within the gel, but in the case of gels formed from branched PAs containing one RGDS epitope, 77% of the cells observed over the course of the experiment migrate through the gel. Similar migration patterns were observed on all other branched PA gels. Cell migration was inhibited when MDA 231 cells were encapsulated in gels formed from linear PA molecules (Fig. 6(B)). Over the course of the experiment, the cells remain rounded, unable to extend long processes and essentially spin locally.

As cell migration is highly dependent on the mechanical properties of the substrate, we carried out oscillating rheometry studies to examine the stiffness of gels formed by branched and linear PA molecules. All gels showed viscoelastic behavior, with $G' > G''$ (Fig. 7). Branched PAs containing cyclic RGDS and linear PA had similar G' values (120 and 106 Pa, respectively), despite the lack of cell migration observed in the linear PA gels. This suggests that poor epitope accessibility in nanofibers containing linear PAs could be contributing to the lack of cell migration in these systems. Branched PAs containing one or two linear RGDS sequences also had similar G' values (37 and 22 Pa), but these values were an order of magnitude lower than those for gels formed by branched PAs containing cyclic RGDS or linear RGDS PAs. In 2D studies, increasing material stiffness has been shown to increase cell migration (although very stiff materials may inhibit migration), [56–59] but in the case of gels formed from branched PA molecules, a change in cell migration is not observed as stiffness increases, and the stiff gels formed from linear PAs cannot support cell migration. At the same time, in gels containing branched PA nanofibers, the dynamics and accessibility of the signals may be enhancing migration in spite of the lower modulus of the matrix they form. These results indicate that 3D cell migration is not simply a function of bulk mechanical properties of the artificial matrix but can also be mediated by supramolecular details affecting its interactions with cells. Geiger has proposed a continuum model for cell adhesion and migration with rigidity, molecular complexity, and three dimensionality plotted on the *x*-, *y*-, and *z*-axes [60]. The behavior of cells will depend on where a material lies within this space, and it is likely that a different phase diagram will need to be developed for each pair involving a specific type of cell and a molecularly designed matrix. By investigating this phase space, we may be able to begin to rationally design materials at the supramolecular level to elicit specific cellular responses.

4. Conclusions

This work has demonstrated the possibility of signaling cells using supramolecular nanofibers displaying cell adhesion epitopes at the extremely high densities associated with van der Waals packing of molecules. Using branched architectures in the molecules that form the nanostructures, greater epitope accessibility to cells at high density can be achieved given their lower packing efficiency and thus additional space for epitope motion. We have observed differential biological cell adhesion and spreading, focal adhesion formation, as well as migration in

a three-dimensional artificial matrix when supramolecular nanostructures display mobile epitopes at high density. The use of artificial matrices with high epitope densities could facilitate receptor clustering for signaling and also maximize successful binding between ligands and receptors. Supramolecular design of artificial extracellular matrices to tune cell response may prove to be a powerful strategy in regenerative medicine.

Acknowledgments

S.I. Stupp is supported by the Department of Energy through Grant DOE DE-FG02-00ER45810, and the National Institutes of Health through Grants NIH 1 R01 DE015920 and NIH 5 R01 EB003806.

B. Geiger holds the Erwin Neter Chair in Cell and Tumor Biology and is supported by grants from the Israel Science foundation, the NIH NanoMedicine Center for Mechanical Biology and the Volkswagen Foundation.

References

[1] Erez N, Bershadsky A, Geiger B. Signalling from adherens-type junctions. Eur J Cell Biol 2005;84:235–44.
[2] Zaidel-Bar R, Cohen M, Addadi L, Geiger B. Heirarchical assembly of cell–matrix adhesion complexes. Biochem Soc Trans 2004;32: 416–20.
[3] Giancotti FG, Rouslahti E. Integrin signalling. Science 1999;295: 1028–33.
[4] Zhu X, Assoian RK. Integrin-dependent activation of MAP kinase: a link to shape-dependent cell proliferation (vol 6, pg 273, 1995). Mol Biol Cell 1996;7(6):1001.
[5] Yamada KM, Even-Ram S. Integrin regulation of growth factor receptors. Nat Cell Biol 2002;4:E75–6.
[6] Takagi J, Springer TA. Integrin activation and structural rearrangement. Immun Rev 2002;186:141–63.
[7] Schwartz MA, Ginsberg MH. Networks and crosstalk: integrin signalling spreads. Nat Cell Biol 2002;4:E65–8.
[8] Liu S, Calderwood DA, Ginsberg MH. Integrin cytoplasmic domain-binding proteins. J Cell Sci 2000;113:3563–71.
[9] Miranti CK, Brugge JS. Sensing the environment: a historical perspective on integrin signal transduction. Nat Cell Biol 2002;4: E83–90.
[10] Desimone DW, Stepp MA, Patel RS, Hynes RO. The integrin family of cell-surface receptors. Biochem Soc Trans 1987;15(5):789–91.
[11] Desimone DW, Stepp MA, Patel R, Marcantonio E, Hynes RO. Integrin structure, function, and developmental expression. Biol Bull 1987;173(3):564.
[12] Desimone DW, Stepp MA, Fonda D, Hynes RO. Structural and functional analyses of integrin, a glycoprotein complex linking fibronectin to the cytoskeleton. J Cell Biol 1986;103(5):A287.
[13] Eliceiri BP. Integrin and growth factor receptor crosstalk. Circ Res 2001;89(12):1104–10.
[14] Hynes RO, Lively JC, McCarty JH, Taverna D, Francis SE, Hodivala-Dilke K, et al. The diverse roles of integrins and their ligands in angiogenesis. Cold Spring Harbor Symp Quant Biol 2002;67:143–53.
[15] Pierschbacher MD, Ruoslahti E. Cell attachment activity of fibronectin can be duplicated by small synthetic fragments of the molecule. Nature 1984;309:30–3.
[16] Pierschbacher MD, Ruoslahti E. Variants of the cell recognition site of fibronectin that retain attachment-promoting activity. Proc Nat Acad Sci USA 1984;81:5985–8.
[17] Anderson JM, Shive M. Biodegradation and biocompatibility of PLA and PLGA microspheres. Adv Drug Del Rev 1997;28(1):5–24.
[18] Putnam A, Mooney DJ. Nat Med 1996;2:824–6.
[19] Drury JL, Mooney DJ. Hydrogels for tissue engineering: scaffold design variables and applications. Biomaterials 2003;24:4337–51.
[20] Pratt AB, Weber FE, Schmoekel HG, Muller R, Hubbell JA. Synthetic extracellular matrices for in situ tissue engineering. Biotechnol Bioeng 2004;86(1):27–36.
[21] Rizzi SC, Hubbell JA. Recombinant protein–co-PEG networks as cell-adhesive and proteolytically degradable hydrogel matrixes. Part I: development and physicochemical characteristics. Biomacromolecules 2005;6(3):1226–38.
[22] Schense JC, Hubbell JA. Cross-linking exogenous bifunctional peptides into fibrin gels with factor XIIIa. Bioconjug Chem 1999; 10(1):75–81.
[23] Hern DL, Hubbell JA. Incorporation of adhesion peptides into nonadhesive hydrogels useful for tissue resurfacing. J Biomed Mater Res 1998;39:266–76.
[24] Hersel U, Dahmen C, Kessler H. RGD modified polymers: biomaterials for stimulated cell adhesion and beyond. Biomaterials 2003;24(24):4385–415.
[25] Dillow AK, Ochsenhirt SE, McCarthy JB, Fields GB, Tirrell M. Adhesion of a5b1 receptors to biomimetic substrates constructed from peptide amphiphiles. Biomaterials 2001;22:493–1505.
[26] Drumheller PD, Hubbell JA. Polymer networks with grafted cell adhesion peptides for highly biospecific cell adhesive substrates. Anal Biochem 1994;222:380–8.
[27] Hubbell JA, Massia SP, Drumheller PD. Surface-grafted cell-binding peptides in tissue engineering of the vascular graft. Ann NY Acad Sci 1992;665:253–8.
[28] Massia SP, Hubbell JA. An RGD spacing of 440 nm is sufficient for integrin avb3-mediated fibroblast spreading and 140 nm for focal contact and stress fiber formation. J Cell Biol 1991;114:1089–100.
[29] Arnold M, Cavalcanti-Adam E, Glass R, Blummel J, Eck W, Kantlehner M, et al. Activation of integrin function by nanopatterned adhesive interfaces. Chem Phys Chem 2004;5:383–8.
[30] Cavalcanti-Adam E, Micoulet A, Blummel J, Kessler H, Spatz J. Lateral spacing of integrin ligands influences cell spreading and focal adhesion assembly. Eur J Cell Biol 2006;85:219–24.
[31] Rowley JA, Mooney DJ. Alginate type and RGD density control myblast phenotype. J Biomed Mater Res 2002;60:217–23.
[32] Berg MC, Yang SY, Hammond PT, Rubner MF. Controlling mammalian cell interactions on patterned polyelectrolyte multilayer surfaces. Langmuir 2004;20:1362–8.
[33] Mann BK, Tsai AT, Scott-Burden T, West JL. Modification of surfaces with cell adheion peptides alters extracellular matrix deposition. Biomaterials 1999;20:2281–6.
[34] Rezania A, Healy KE. The effect of peptide surface density on mineralization of a matrix deposited by osteogenic cells. J Biomed Mater Res 2000;52:595–600.
[35] Maheshwari G, Brown G, Lauffenburger DA, Wells A, Griffith LG. Cell adhesion and motility depend on nanoscale RGD clustering. J Cell Sci 2000;113:1677–86.
[36] Lee KY, Alsberg E, Hsiong S, Comisar W, Linderman J, Ziff R, et al. Nanoscale adhesion ligand organization regulates osteoblast proliferation and differentiation. Nano Lett 2004;4:1501–6.
[37] Chen CS, Ostuni E, Whitesides GM, Ingber DE. Using self-assembled monolayers to pattern ECM proteins and cells on substrates. Methods Mol Biol 2000;139:209–19.
[38] Mrksich M, Whitesides GM. Using self-assembled monolayers to understand interactions of man-made surfaces with proteins and cells. Ann Rev Biophys Biomol Struct 1996;25:55–78.
[39] Hartgerink JD, Beniash E, Stupp SI. Self-assembly and mineralization of peptide-amphiphile nanofibers. Science 2001;294(5547): 1684–8.
[40] Hartgerink JD, Beniash E, Stupp SI. Peptide-amphiphile nanofibers: a versitile scaffold for the preparation of self-assembling materials. Proc Nat Acad Sci USA 2002;99(8):5133–8.

[41] Niece KL, Hartgerink JD, Donners JJJM, Stupp SI. Self-assembly combining two bioactive peptide-amphiphile molecules into nanofibers by electrostatic interaction. J Am Chem Soc 2003;125:7146–7.
[42] Beniash E, Hartgerink JD, Storrie H, Stupp SI. Self-assembling peptide amphiphile nanofiber matrices for cell entrapment. Acta Biomater 2005;1:387–97.
[43] Silva GA, Czeisler C, Niece KL, Beniash E, Harrington DA, Kessler JA, et al. Selective differentiation of neural progenitor cells by high-epitope density nanofibers. Science 2004;303(5662):1352–5.
[44] Guler MO, Soukasene S, Hulvat JF, Stupp SI. Presentation and recognition of biotin on nanofibers formed by branched peptide amphiphiles. Nano Lett 2005;5(2):249–52.
[45] Guler MO, Hsu L, Soukasene S, Harrington DA, Hulvat JF, Stupp SI. Presentation of RGDS epitopes on self-assembled nanofibers of branched peptide-amphiphiles. Biomacromolecules 2006;7:1855–63.
[46] Pierschbacher MD, Ruoslahti E. Influence of stereochemistry of the sequence Arg-Gly-Asp-Xaa on binding specificity in cell adhesion. J Biol Chem 1987;262:17294–8.
[47] Sastry S, Burridge K. Focal adhesions: a nexus for intracellular signalling and cytoskeletal dynamics. Exp Cell Res 2000;261:25–36.
[48] Galbraith CG, Yamada KM, Sheetz MP. The relationship between force and focal compex development. J Cell Biol 2002;159:695–705.
[49] Zamir E, Geiger B. Components of cell–matrix adhesions. J Cell Sci 2001;114:3577–9.
[50] Pierschbacher MD, Hayman EG, Ruoslahti E. The cell attachment determinant in fibronectin. J Cell Biochem 1985;28(2):115–26.
[51] Harrington DA, Cheng EY, Guler MO, Lee LK, Donovan JL, Claussen RC, et al. Branched peptide-amphiphiles as self-assembling coatings for tissue engineered scaffolds. J Biomed Mater Res A 2006;5(2):249–52.
[52] Behanna HA, Donners JJ, Gordon AC, Stupp SI. Coassembly of amphiphiles with opposite peptide polarities into nanofibers. J Am Chem Soc 2005;127(4):1193–200.
[53] Houseman BT, Mrksich M. The microenvironment of immobilzed Arg-Gly-Asp peptides is an important determinant of cell adhesion. Biomaterials 2001;22:943–55.
[54] Kato M, Mrksich M. Using model substrates to study the dependence of focal adhesion formation on the affinity of integrin–ligand complexes. Biochemistry 2004;43:2699–707.
[55] Wolf K, Mazo I, Leung H, Engelke K, von Andrian U, Deryugina E, et al. Compensation mechanism in tumor cell migration: mesenchymal–amoeboid transition after blocking of pericellular proteolysis. J Cell Biol 2003;160(2):267–77.
[56] Lo C-M, Wang H-B, Dembo M, Wang Y-L. Cell movement is guided by the rigidity of the substrate. Biophys J 2000;79:144–52.
[57] Wong JY, Velasco A, Rajogopalan P, Pham Q. Directed movement of vascular smooth muscle cells on gradient-compliant hydrogels. Langmuir 2003;19:1908–13.
[58] Engler A, Bacakova L, Newman C, Hategan A, Griffin M, Discher D. Substrate compliance versus ligand density in cell on gel responses. Biophys J 2004;86:617–28.
[59] Schense JC, Hubbell JA. Three-dimensional migration of neurites is mediated by adhesion site density and affinity. J Biol Chem 2000; 275:6813–8.
[60] Geiger B. Encounters in space. Science 2001;294:1661–3.